

Imaging quasiparticle wave functions in quantum dots via tunneling spectroscopy

Massimo Rontani and Elisa Molinari

INFN National Research Center on nanoStructures and bioSystems at Surfaces (S3), and Dipartimento di Fisica, Università degli Studi di Modena e Reggio Emilia, Via Campi 213/A, 41100 Modena, Italy

(Received 21 March 2005; published 30 June 2005)

We show that in quantum dots the physical quantities probed by local tunneling spectroscopies—namely, the quasiparticle wave functions of interacting electrons—can considerably deviate from their single-particle counterparts as an effect of Coulomb correlation. From the exact solution of the few-particle Hamiltonian for prototype dots, we find that such deviations are crucial to predict wave function images at low electron densities or high magnetic fields.

DOI: 10.1103/PhysRevB.71.233106

PACS number(s): 73.21.La, 73.20.Qt, 73.23.Hk, 73.63.Kv

Current single-electron tunneling spectroscopies in semiconductor quantum dots^{1–3} (QD's) may provide spectacular images of the QD wave functions, in both real^{4–6} and reciprocal space.^{7–9} The measured intensities have been generally attributed to the probability densities of ground or excited single-electron states occupying the dot. As pointed out by Wibbelhoff *et al.*,⁹ however, the role of other electrons filling the dot may actually be relevant. Indeed, QD's can be strongly interacting objects with a completely discrete energy spectrum, which in turn depends on the number of electrons,^{1,3} N . Therefore, orbitals can be ill defined, losing their meaning due to interactions. Also, it is unclear how many electrons one should take into account to calculate the total density of states, as a particle tunnels into a QD filled with N electrons. In this paper we thus address the following basic questions: What are the physical quantities that are actually probed by the scanning tunneling microscopy^{4–6} (STM) or magnetotunneling spectroscopy^{7–9} of QD's? How do they depend on interactions? Can they deviate from the common single-particle picture in physically relevant regimes? If only one many-body state is probed at a time, then the signal is proportional to the probability density of the *quasiparticle* (QP) being injected into the interacting QD. We demonstrate that the QP density dramatically depends on the strength of correlation inside the dot and predict the wave function mapping to be a useful experimental tool to image QP's, in both direct and reciprocal space.

The imaging experiments, in their essence, measure quantities directly proportional to the probability for transfer of an electron through a barrier, from an emitter, where electrons fill in a Fermi sea, to a dot, with completely discrete energy spectrum. In multiterminal setups one can neglect the role of electrodes other than the emitter, to a first approximation. The measured quantity can be the current,^{4,7} the differential conductance,^{5,6,8,10} or the QD capacitance,^{9,11} while the emitter can be the STM tip^{4–6} or a n -doped GaAs contact,^{7–11} and the barrier can be the vacuum^{4–6} as well as a AlGaAs spacer.^{7–11}

According to the seminal paper by Bardeen,¹² the transition probability (at zero temperature) is given by the expression $(2\pi/\hbar)|\mathcal{M}|^2 n(\epsilon_f)$, where \mathcal{M} is the matrix element and $n(\epsilon_f)$ is the energy density of the final QD states. Common wisdom would predict the probability to be proportional to

the total density of QD states at the resonant tunneling energy ϵ_f , possibly space-resolved since \mathcal{M} would depend on the resonant QD orbital.¹³ To proceed, let us assume that electrons from the emitter access through the barrier a single QD at a sharp resonant energy, corresponding to a unique, well-defined many-body QD state, and reconsider the transition matrix element $\mathcal{M}_{k,N}$ for transfer of an electron from emitter to QD. $\mathcal{M}_{k,N}$ is given by [recasting Eqs. (6) and (7) of Ref. 12 in second-quantized form]

$$\mathcal{M}_{k,N} \propto \langle \{k\}, N-1 | \hat{\mathcal{M}} | \{k^*\}, N \rangle, \\ \hat{\mathcal{M}} = \frac{\hbar^2}{2m^*} \int \left[\hat{\Psi}^\dagger \frac{\partial \hat{\Psi}}{\partial z} - \frac{\partial \hat{\Psi}^\dagger}{\partial z} \hat{\Psi} \right] \delta(z_{\text{bar}} - z) d\tau. \quad (1)$$

Here $|\{k\}, N-1\rangle$ and $|\{k^*\}, N\rangle$ are two many-particle states of the entire system of similar energies, with $N-1$ and N interacting electrons in the QD, respectively, and the remaining $N_{\text{tot}}-N+1$ and $N_{\text{tot}}-N$ electrons, respectively, in the emitter. The fixed coordinate along the tunneling direction z appearing in Eq. (1), z_{bar} , can be everywhere in the barrier, and $d\tau$ is the infinitesimal volume element. The fermionic field operator $\hat{\Psi}(\mathbf{r})$, destroying an electron at position $\mathbf{r} = (\varrho, z)$, can be expanded over the basis of emitter and QD single-particle states ϕ_k and ϕ_α , respectively:¹⁴ $\hat{\Psi}(\mathbf{r}) = \sum_i \phi_i(\mathbf{r}) \hat{c}_i$, where $i = k, \alpha$ and we take unitary volume normalization. We omit spin indexes and summations for the sake of simplicity. We assume that electrons in the emitter do not interact and are associated with the two sets of quantum numbers $\{k\}$ and $\{k^*\}$, respectively, which differ in the occurrence of the index k labeling the electron which leaves the emitter and tunnels to the QD as $|\{k\}, N-1\rangle$ evolves to $|\{k^*\}, N\rangle$. Moreover, we assume for convenience that the xy and z motions of electrons are separable and that electrons in the QD all occupy the same confined single-particle state along z , $\chi_{\text{QD}}(z)$: namely, $\phi_\alpha(\mathbf{r}) = \phi_\alpha(\varrho) \chi_{\text{QD}}(z)$. Under these conditions we may factorize the matrix element as $\mathcal{M}_{k,N} \propto T_k M_{k,N}$, with

$$T_k = \frac{\hbar^2}{2m^*} \left[\chi_k^*(z) \frac{\partial \chi_{\text{QD}}(z)}{\partial z} - \chi_{\text{QD}}(z) \frac{\partial \chi_k^*(z)}{\partial z} \right]_{z=z_{\text{bar}}}, \quad (2)$$

where $\chi_k(z)$ is the emitter state along z evanescent in the barrier, $\phi_k(\mathbf{r}) = \phi_k(\varrho) \chi_k(z)$, and

$$M_{k,N} = \sum_{\alpha} \int \phi_k^*(\varrho) \phi_{\alpha}(\varrho) d\varrho \langle \{k\}, N-1 | \hat{c}_k^{\dagger} \hat{c}_{\alpha} | \{k^*\}, N \rangle.$$

Eventually assuming that the many-body states can be factorized into an emitter and a QD part, we obtain

$$M_{k,N} = \int \phi_k^*(\varrho) \varphi_{\text{QD}}(\varrho) d\varrho, \quad (3)$$

where $\varphi_{\text{QD}}(\varrho)$ is the QP wave function of the interacting QD system:¹⁵

$$\varphi_{\text{QD}}(\varrho) = \langle N-1 | \hat{\Psi}(\varrho) | N \rangle. \quad (4)$$

The results (3) and (4) are the key for predicting wave function images in both real and reciprocal space. In STM, $\phi_k(\varrho)$ is the localized tip wave function; if we ideally assume it pointlike and located at ϱ_0 ,¹³ i.e., $\phi_k(\varrho) \approx \delta(\varrho - \varrho_0)$, then the signal intensity is proportional to $|\varphi_{\text{QD}}(\varrho_0)|^2$, which is the usual result of the one-electron theory,^{6,13} provided the ill-defined QD orbital is replaced by the QP wave function unambiguously defined by Eq. (4). In magnetotunneling spectroscopy, the emitter in-plane wave function is a plane wave, $\phi_k(\varrho) = e^{ik \cdot \varrho}$, and the matrix element (3) is the Fourier transform of φ_{QD} , $M_{k,N} = \varphi_{\text{QD}}(\mathbf{k})$. Again, we generalize the standard one-electron result by substituting $\varphi_{\text{QD}}(\mathbf{k})$ for the QD orbital [then Eqs. (3) and (2) coincide with (A1) and (A2) of Ref. 8]. Note that $M_{k,N}$ is the relevant quantity also for intensities in space-integrated spectroscopies probing the QD addition energy spectrum.^{10,11} Consistently, in the non-interacting case, $\varphi_{\text{QD}}(\varrho)$ reduces to the highest-occupied one-electron orbital $\phi_{\alpha}(\varrho)$ (Ref. 13): in this limit an electron tunnels from the emitter to the orbital $\phi_{\alpha}(\varrho)$ which resonates at the Fermi energy, with $|N\rangle = \hat{c}_{\alpha}^{\dagger} |N-1\rangle$. The latter regime probably corresponds to most of the existing experimental evidence.⁴⁻⁹ However, it is interesting to analyze realistic scenarios that deviate from the one-electron picture.

Therefore, we study $\varphi_{\text{QD}}(\varrho)$ in a paradigmatic interacting case and consider a few electrons in a two-dimensional harmonic trap, which was proven to be an excellent model for different experimental setups.³ The QD effective-mass Hamiltonian is

$$H = \sum_i^N H_0(i) + \frac{1}{2} \sum_{i \neq j} \frac{e^2}{\kappa |\varrho_i - \varrho_j|}, \quad (5)$$

with

$$H_0(i) = \frac{1}{2m^*} \left[\mathbf{p} - \frac{e}{c} \mathbf{A}(\varrho) \right]^2 + m^* \omega_0^2 \varrho^2 / 2. \quad (6)$$

Here κ is the static relative dielectric constant of the host semiconductor, and $\mathbf{A}(\varrho)$ is the vector potential ($\mathbf{A} = \mathbf{B} \times \varrho / 2$) associated with a static and uniform magnetic field B along z , which reduces the cylindrical spatial symmetry group of the system from $D_{\infty h}$, at $B=0$, to $C_{\infty v}$, when $B \neq 0$, making it chiral. The QD wave function has an azimuthal quantum number m , $\varphi_{\text{QD}}(\varrho) = \varphi_{\text{QD}}(\varrho) e^{im\varphi}$ (ϱ and φ are respectively the modulus and azimuthal angle of ϱ), which is fixed by the total angular momenta M of $|N\rangle$ and

$|N-1\rangle$, $m = M_N - M_{N-1}$, and can be expanded over the basis of Fock-Darwin (FD) orbitals $\varphi_{nm}(\varrho)$,¹ eigenstates of the single-particle Hamiltonian (6): $\varphi_{\text{QD}}(\varrho) = \sum_{n=0}^{\infty} a_n \varphi_{nm}(\varrho)$, where n 's are radial quantum numbers and a_n coefficients to be determined. We solve numerically the few-body problem of Eq. (5), for the ground state at different N 's, by means of the configuration interaction (CI) method,¹⁶ where $|N\rangle$ is expanded in a series of Slater determinants built by filling in the FD orbitals with N electrons and consistently with symmetry constraints.¹⁶ Then, we evaluate the matrix element (4) and find the values of a_n for a truncated FD basis set.

There are two ways of artificially tuning the strength of the Coulomb correlation in QD's: one is to dilute the electron density, and the other is to turn on B . In both cases, at low enough densities or strong enough fields, electrons pass from a "liquid" phase, where low-energy motion is equally controlled by kinetic and Coulomb energy, to a "crystallized" phase, reminiscent of the Wigner crystal in the bulk, where electrons are localized in space and arrange themselves in a geometrically ordered configuration such that electrostatic repulsion is minimized.³

We first consider reducing the density at $B=0$. The typical QD lateral extension is given by the characteristic dot radius $\ell_{\text{QD}} = (\hbar / m^* \omega_0)^{1/2}$, ℓ_{QD} being the mean-square root of ϱ on the FD lowest-energy level φ_{00} . As we keep N fixed and increase ℓ_{QD} , the Coulomb-to-kinetic energy ratio $\lambda = \ell_{\text{QD}} / a_B^*$ [$a_B^* = \hbar^2 \kappa / (m^* e^2)$ is the effective Bohr radius of the dot] (Ref. 18) increases as well, driving the system into the "Wigner" regime.¹⁹ As a rough indication, consider that for $\lambda \approx 2$ or lower the electronic ground state is liquid, while above $\lambda \approx 4$ electrons form a crystallized phase.¹⁸

Figure 1 shows φ_{QD} vs ϱ , as up to six electrons are successively injected into a liquid QD with a realistic density of $\lambda = 2$.¹⁰ The QD filling sequence is well known,^{10,11} in analogy with the Aufbau principle of atomic physics: in the independent-electron picture ($\lambda = 0$, dashed lines), φ_{QD} is the highest-energy occupied orbital which is filled by the electron added to the dot. However, Coulomb correlation significantly spreads the wave function (solid lines) and moves the QP peak towards the QD edge. The spreading is caused by the increase of weights a_n of high-energy FD orbitals, as the interaction is turned on; nevertheless, the behavior of φ_{QD} around $\varrho \approx 0$ is dictated by its angular dependence, $\varphi_{\text{QD}}(\varrho) \propto \varrho^{|m|}$, while it decays like $\exp(-\varrho^2 / 2\ell_{\text{QD}}^2)$ as $\varrho \rightarrow \infty$. The QP amplitude is strongly suppressed in the $(N-1) \rightarrow N$ tunneling processes involving the $N=4$ open-shell ground state, with respect to other additions (Fig. 1). This is a spin-blockade effect, since the total spin S is maximum at $N=4$ ($S=1$ according to Hund's rule¹⁰), and we assume that its z component is zero, $S_z=0$. Besides, the general trend is that the QP wave function norm and, hence, the integrated experimental signal diminish as N and λ increase (see also Fig. 2).

Note that the interpretation of tunneling spectroscopy in terms of the total density, $n(\varrho) = \langle N | \hat{\Psi}^{\dagger}(\varrho) \hat{\Psi}(\varrho) | N \rangle / N$, is inconsistent with our point of view, as is seen by comparing the QP wave functions of Fig. 1 with the total densities for the corresponding N -electron states (insets). While the total densities and QP probabilities resemble each other up to the

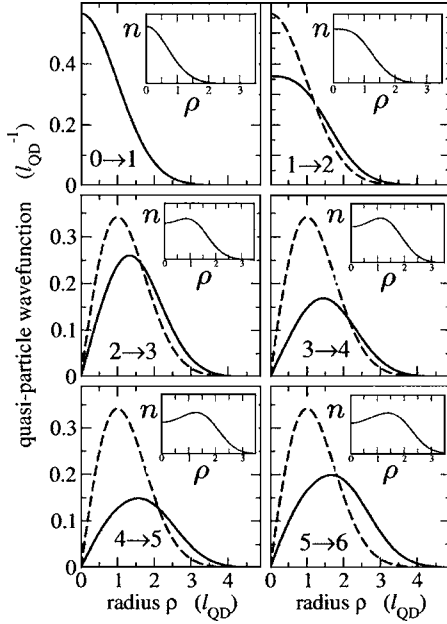


FIG. 1. Quasiparticle wave function (solid line) vs ϱ for different $(N-1) \rightarrow N$ transitions, with $\lambda=2$. The dashed line represents the noninteracting orbital ($\lambda=0$). The ground states are $(M, S) = (0, 1/2), (0, 0), (1, 1/2), (0, 1), (1, 1/2), (0, 0)$, for N going from 1 to 6, respectively. $S_z=0$ ($S_z=1/2$) if N is even (odd). The norm of the $\lambda=2$ wave function is 1.0, 0.84, 0.84, 0.40, 0.37, 0.73, respectively. Insets: total ground-state charge densities $n(\varrho)$ (arb. units) for N going from 1 (top left) to 6 (right bottom). The length unit is ℓ_{QD} .

addition of the second electron, after the third electron tunnels into the dot they can be clearly discriminated in the laboratory: QP probabilities have a strong angular dependence (hybridizing degenerate states with $\pm m$) and a node at the QD center, while total densities are approximately circular (exactly, for $N=4, 6$) and filled.

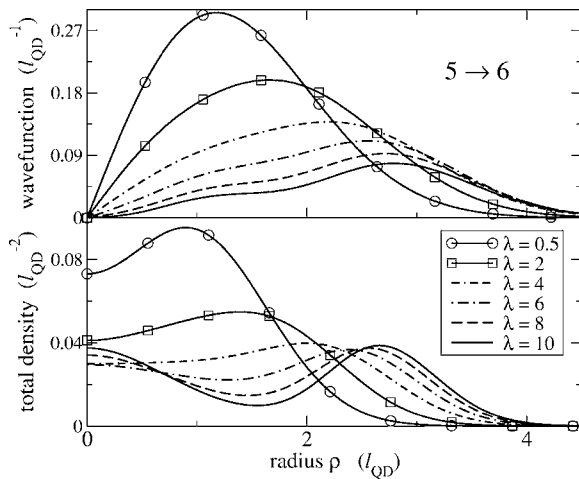


FIG. 2. Top: quasiparticle wave function vs ϱ for different values of λ , as the sixth electron tunnels into the QD. The wave function norm, for λ going from 0.5 to 10, is 0.97, 0.73, 0.48, 0.32, 0.22, 0.15, respectively. Bottom: six-electron total density $n(\varrho)$ vs ϱ . The ground states for $N=5, 6$ are $(M, S) = (1, 1/2), (0, 0)$, respectively, for all λ .

As one reduces the density, the appearance of QP wave functions dramatically changes. In Fig. 2 we study the injection of the sixth electron, as λ goes from 0.5 up to 10. Note that $\lambda=0.5, 2, 4$ (equivalent to GaAs lateral confinement energies $\hbar\omega_0=47, 3.0, 0.74$ meV, respectively) typically correspond to different experimental QD devices, such as self-assembled,^{8,20} vertical mesa-etched,¹⁰ and 2DEG-depletion QD's.¹¹ A six-electron Wigner molecule forms for $\lambda > 4$, with one electron localized at the QD center and the remaining five arranged on an outer ring, at the vertices of a regular pentagon.^{18,21,22} The crystallization is clearly seen in the bottom panel of Fig. 2, where, as λ increases, the total density develops one peak at $\varrho=0$, for the central electron, and another one, close to $\varrho=3\ell_{\text{QD}}$, for the outer ring. Similarly, the five-electron molecule is a hollow pentagon.^{18,21} In the top panel of Fig. 2 we see that the QP wave function is strongly affected by electron localization: while for $\lambda < 4$ it somehow resembles the noninteracting FD orbital $(n, m) = (0, -1)$, being spread uniformly across the dot, for $\lambda > 4$ it develops a well-formed peak close to the outer-ring position. The QP weight in the region inside the ring is strongly depleted, eventually appearing as a shoulder of the main peak. We conclude that, in the crystallized phase, the sixth electron can only enter the external ring, with negligible probability of being located in the center. For smaller N , we find that electrons just enter the outer ring, since the pertinent geometrical phases are hollow regular polygons.²³

We now come to the effect of a strong magnetic field parallel to the tunneling direction z . As B increases, the kinetic energy is quenched, Landau bands of almost degenerate FD levels being formed. M increases due to Coulomb repulsion, since the higher m , the outer the FD orbital.²⁴ In correspondence of “magic” values of M , the ground state turns out to be particularly stable:²⁴ this family of incompressible²⁵ states has been variously regarded as reminiscent of the fractional quantum Hall effect (FQHE) states in two-dimensional electron layers³ or as a collection of Wigner molecules.²⁶

In analogy with the FQHE, it is convenient to introduce the filling factor ν , defined as $\nu=N(N-1)/2M$, and to consider only FD levels in the lowest Landau band and full spin polarization, which turns out to be a reasonable approximation at high B .³ In realistic situations, there are significant B ranges where ν is constant as N is changed.^{3,27} At $\nu=1$, the interacting states are maximum density droplets,^{3,28} namely, incompressible disks of almost uniform density, $|N\rangle = \prod_{m=0}^{N-1} \hat{c}_{0m}^\dagger |0\rangle$, and φ_{QD} is simply the highest occupied FD state, φ_{0N-1} , located at the edge of the dot, which is being filled by the tunneling electron, with $a_n = \delta_{n0}$:

$$\varphi_{\text{QD}}(\varrho) = \varphi_{n=0, m=N-1}(\varrho). \quad (7)$$

Equation (7) is a remarkable result: while the total electron density is a uniform disk, the measured squared modulus of QP wave function will be an annulus of the same radius as the charge distribution. If $\nu < 1$, the wave function will be still proportional to the FD orbital $\varphi_{n=0, m}$, with $m=(N-1)/\nu$ and $a_0 \neq 1$: namely, $\varphi_{\text{QD}}(\varrho) = a_0 \varphi_{n=0, m}(\varrho)$. The only effect of strong correlation in these regimes is to modulate the amplitude of the noninteracting wave function via the coefficient a_0 . Table I shows the calculated values of a_0

TABLE I. Absolute value of the modulation coefficient $|a_0|$ of the quasiparticle wave function $\varphi_{\text{QD}}(\mathcal{Q})=a_0\varphi_{0m}(\mathcal{Q})$, where $m=(N-1)/\nu$, for different $(N-1)\rightarrow N$ tunneling processes and filling factors ν .

$(N-1)\rightarrow N$	$\nu=1$	$\nu=1/2$	$\nu=1/3$	$\nu=1/4$	$\nu=1/5$
1 \rightarrow 2	1.00	1.00	0.500	0.707	0.250
2 \rightarrow 3	1.00	0.430	0.336	0.190	0.106
3 \rightarrow 4	1.00	0.520	0.270	0.201	0.0649
4 \rightarrow 5	1.00	0.158	0.239	0.0650	0.0507
5 \rightarrow 6	1.00	0.294	0.210	0.0541	0.0274

for various tunneling processes at particularly stable filling factors. Except for some cases, $|a_0|$ monotonously decreases as ν diminishes or as N increases. E.g., at $\nu=1/5$, $|a_0|$ is reduced by two order of magnitudes with respect to $\nu=1$, when the sixth electron enters the dot. Table I shows that interaction enforces very effectively the orthogonality of incompressible states,²⁹ and therefore we expect that, as a high-field component is applied parallel to z , tunneling is strongly suppressed by the reduction of the matrix element $M_{k,N}$ [Eq. (3)]: a purely many-body mechanism, the single-particle matrix element T_k [Eq. (2)] being left unchanged by the field.

The loss of QP weight as either λ (Figs. 1 and 2) or B

(Table I) increases is a general signature of Coulomb correlation. As the electron puddle becomes more correlated, its total wave function acquires new different Slater determinant components to reduce its Coulomb energy. Such new components in general do not contribute to the coefficients a_n of the QP wave function.

In conclusion, we have shown that quasiparticle wave functions of QD's are extremely sensitive to electron-electron correlation and may differ from single-particle states in physically relevant cases. This result is of interest to predict the real- and reciprocal-space wave function images obtained by tunneling spectroscopies, as well as the intensities of addition spectra of QD's. Close comparison with experiment is not yet possible in the case of Ref. 9, where many dots are probed at once and the confinement is too strong. Promising samples are also those of Refs. 10 and 11, allowing for access to a single dot and full control of N . We hope that our results will stimulate further experiments. We believe that our findings will be important also for other strongly confined systems, like, e.g., nanostructures at surfaces.³⁰

We thank O. S. Wibbelhoff and A. Lorke for inspiring discussions. This paper is supported by MIUR-FIRB RBAU01ZEML, MIUR-COFIN 2003020984, I.T. INFN Calc. Par. 2004-2005, MAE-DGPCC.

- ¹L. Jacak, P. Hawrylak, and A. Wójs, *Quantum Dots* (Springer, Berlin, 1998).
²D. Bimberg, M. Grundmann, and N. N. Ledentsov, *Quantum Dot Heterostructures* (Wiley, New York, 1999).
³S. M. Reimann and M. Manninen, *Rev. Mod. Phys.* **74**, 1283 (2002).
⁴B. Grandidier *et al.*, *Phys. Rev. Lett.* **85**, 1068 (2000).
⁵O. Millo *et al.*, *Phys. Rev. Lett.* **86**, 5751 (2001).
⁶T. Maltezopoulos *et al.*, *Phys. Rev. Lett.* **91**, 196804 (2003).
⁷E. E. Vdovin *et al.*, *Science* **290**, 122 (2000).
⁸A. Patanè *et al.*, *Phys. Rev. B* **65**, 165308 (2002).
⁹O. S. Wibbelhoff *et al.*, *Appl. Phys. Lett.* **86**, 092104 (2005).
¹⁰S. Tarucha *et al.*, *Phys. Rev. Lett.* **77**, 3613 (1996).
¹¹R. C. Ashoori, *Nature (London)* **379**, 413 (1996).
¹²J. Bardeen, *Phys. Rev. Lett.* **6**, 57 (1961).
¹³J. Tersoff and D. R. Hamann, *Phys. Rev. B* **31**, 805 (1985); J. Tersoff, *Phys. Rev. Lett.* **57**, 440 (1986).
¹⁴ ϕ_k and ϕ_α are not mutually orthogonal, since they are not eigenstates of the whole system Hamiltonian (Ref. 12).
¹⁵The quantity is also known as the spectral density amplitude of the one-electron propagator resolved in real space: for analogous treatments in many-body tunneling theory see, e.g., J. A. Appelbaum and W. F. Brinkman, *Phys. Rev.* **186**, 464 (1969); T. E. Feuchtwang, *Phys. Rev. B* **10**, 4121 (1974), and refs. therein.
¹⁶For details on our CI approach see Ref. 17. Here we implemented a parallel version of our CI code, allowing for using a FD basis set as large as 36 orbitals and for diagonalizing matrices of

- linear dimensions up to $\approx 10^6$. As a convergence test, we could accurately reproduce QMC ground state energies up to $\lambda=8$ and $N=6$ (Ref. 18).
¹⁷M. Rontani *et al.*, *Phys. Rev. B* **69**, 085327 (2004).
¹⁸R. Egger *et al.*, *Phys. Rev. Lett.* **82**, 3320 (1999).
¹⁹The dimensionless ratio λ is the QD analog to the density parameter r_s in extended systems.
²⁰M. Fricke *et al.*, *Europhys. Lett.* **36**, 197 (1996).
²¹F. Bolton and U. Rössler, *Superlattices Microstruct.* **13**, 139 (1993); V. M. Bedanov and F. M. Peeters, *Phys. Rev. B* **49**, 2667 (1994).
²²M. Rontani *et al.*, *Europhys. Lett.* **58**, 555 (2002).
²³There is a complication for the 3 \rightarrow 4 process, since, for λ between 4 and 6, the three-electron ground state becomes fully spin polarized (Ref. 18) and the symmetry of the QP wave function changes from $m=-1$ to $m=0$. Correspondingly, the 2 \rightarrow 3 channel is fully spin blocked.
²⁴P. A. Maksym *et al.*, *Phys. Rev. Lett.* **65**, 108 (1990).
²⁵R. B. Laughlin, *Phys. Rev. B* **27**, 3383 (1983).
²⁶See, e.g., P. A. Maksym *et al.*, *J. Phys.: Condens. Matter* **12**, R299 (2000), and references therein.
²⁷T. H. Oosterkamp *et al.*, *Phys. Rev. Lett.* **82**, 2931 (1999).
²⁸A. H. MacDonald *et al.*, *Aust. J. Phys.* **46**, 345 (1993).
²⁹C. Yannouleas *et al.*, *Phys. Rev. B* **68**, 035326 (2003).
³⁰See, e.g., P. Jarillo-Herrero *et al.*, *Nature (London)* **429**, 389 (2004).